JMEPEG (2007) 16:614–619
DOI: 10.1007/s11665-007-9039-x

1059-9495/$19.00

Effect of Aluminizing and Nitridation on the Oxidation Behavior of AISI 316LN SS

S. Rajendran Pillai, Harish Singh Chandel, R.K. Dayal, R.V. Subba Rao, and H.S. Khatak

(Submitted January 10, 2006; in revised form May 15, 2006)

The application of stainless steel at temperatures above 973 K is rendered difficult by the chromium loss due to generation of volatile CrO_3 species and the consequent reduction in the capacity to maintain protective scale. We have attempted a method to circumvent this problem by modifying the surface. The surface was modified by three techniques each suiting a particular application. The first two methods involved aluminizing the surface by physical vapor deposition as the initial step. The pre-treatments were carried out in two ways viz. (i) high temperature diffusion-annealing and (ii) laser annealing of the surface. In the third method the specimen was modified by ion-nitriding. The oxidation behavior of these modified steels was compared with stainless steel in the as-received condition to exactly gauge the effect of surface modification. The oxidation experiment was carried out at 1123 K for 3.6 Ms. The oxidation was interrupted at specific time intervals to examine the mass change of the specimen and mass of the spalled oxide. The results indicated that aluminizing followed by heat-treatment and laser-treatment showed significant improvement in the adherence of the scale. On the other hand the bare and nitrided specimens showed similar behavior characterized by intermittent spallation and poor adherence. Nitriding resulted in the increase in the surface hardness. The post-oxidation examinations were carried out using SEM, EDAX and GIXRD. The uncoated specimen showed the presence of uniform oxide layer and contained oxides of iron and chromium. The aluminum-coated specimen showed the presence of adherent scale. The surface showed a nodular structure due to the formation of pits and zones of enhanced oxidation. The major part of the oxide was alumina with small fractions of chromium and iron oxides. The nodular region was enriched in the oxide of iron. The analysis of the surface by GIXRD revealed the nature of different phases formed on the surface. The oxide on the oxidized bare metal was Cr_2O_3, aluminized (non-oxidized) AlFe and Al_2Fe, aluminized and oxidized Al_2O_3 and $FeCr_2O_4$, aluminized and laser-treated Al_2O_3, $FeCr_2O_4$, Fe_2O_3 and Fe_3O_4, nitrided Fe_2O_3 and $FeCr_2O_4$. In the light of the above results the mechanism of scale failure has been proposed.

Keywords ion-nitriding, laser annealing, oxidation, physical vapor deposition, surface modification

1. Introduction

Austenitic stainless steels of different grades are widely employed as structural materials in several industrial applications where high temperatures are encountered. The nitrogen substituted low carbon modification is receiving special attention on account of its resistance to pitting and intergranular corrosion coupled with improved creep strength. In some of the fast reactor applications such as sodium immersion heaters this material encounters very high temperatures (873-1073 K) so that oxidation becomes an important mode of material degradation and the consequent loss in mechanical strength. Such a situation of extremely high temperature may also arise in a reactor due to loss of coolant accident. Increasing loss in the cross section due to oxidation becomes a major concern under these conditions.

In order to protect stainless steel from oxidation loss, different methods of surface modifications are reported in the literature (Ref 1-5). In these cases only the modified surface interacts with the high temperature environment and the surface as such is capable of offering endurance against high rate of oxide growth and consequent spallation.

Among the oxide scales, those of aluminum, chromium and silicon are the ones that offer maximum protection against progress of oxidation. Therefore diffusion coatings are generally employed to increase the surface concentration of these elements. The deposit can be applied by either physical vapor deposition or chemical vapor deposition methods (Ref 6-9). Even though alumina scale has been reported to offer best protection, it suffers from poor ductility. In order to render the scale more ductile, modifying elements such as chromium, palladium and platinum are added. This addition is achieved by pre-treatment or co-deposition (Ref 10).

Ion-implantation is an effective method to introduce desired foreign elements into the metallic matrix without involving the rigors of alloy making (Ref 11). In this method, accelerated ions are allowed to impinge on the surface. The depth of penetration is in the range of 0.01-1.0 μm. The radiation damage introduced on the surface is rapidly annealed by heating to high temperature.

S. Rajendran Pillai, R.K. Dayal, R.V. Subba Rao, and **H.S. Khatak,** Corrosion Science and Technology Division, Materials Characterization Group, Indira Gandhi Centre for Atomic Research, Kalpakkam 603 102 Tamil Nadu, India. Contact e-mail: srp@igcar.ernet.in. **Harish Singh Chandel,** Department of Metallurgy and Materials Engineering, Visveswaraya National Institute of Technology, Nagpur 440 011, India.

The application of laser to melt the surface of metal is an important method to bring about tailor made modification to the surface. Laser is capable of heating the surface without subjecting the matrix of the alloy to high temperature.

In the present investigation, the oxidation behavior of AISI 316 LN was studied at 1123 K for 3.6 Ms. The surface of the specimens was modified by three methods;

(i) Aluminizing followed by high temperature pre-treatment.
(ii) aluminizing followed by laser treatment
(iii) ion-nitriding

Aluminizing was carried out by physical vapor deposition method. The paper discusses the effect of these surface treatments by comparing with the oxidation behavior of as-received material. Nitridation was also attempted as surface modification mainly with a view to impart better surface hardness. The effect of nitridation on the high temperature oxidation behavior has been analyzed.

Post-oxidation examinations were carried out using SEM and EDS to identify the nature of the phases formed and to examine the morphology of the surface.

2. Experimental

2.1 Preparation of the Specimen

The composition of the material selected for the investigation is given in Table 1.

The material was cut into sizes of $12 \times 12 \times 3$ mm^3. These were polished using successive grades of silicon carbide-coated paper and finally polished to 1 μm finish using diamond paste. The polished specimens were cleaned ultrasonically followed by the use of acetone.

2.2 Aluminizing

The aluminum coating was carried out using Resistance Heating Evaporation Technique (RHET) coupled with the application of vacuum of 10^{-5} Torr. Aluminum foils of purity 99.99% were used as the source. These foils were attached to a tungsten filament which promoted the evaporation of aluminum and its deposition on the specimen kept inside the vacuum chamber.

2.3 Pre-Treatment of Aluminized Specimen

2.3.1 High Temperature Diffusion-Annealing. High temperature pre-treatment was imparted to aluminized specimen to promote generation of adherent scale. Initially the specimens were heated at 873 K for 10.8 ks to promote the complete oxidation of the deposited aluminum. Subsequently, the specimens were heated at 1173 K for 90 ks. This treatment is to promote the complete conversion of γ-alumina generated initially to the θ-alumina. The θ-alumina undergoes ultimate conversion to α-alumina on prolonged exposure to high temperature. The α-alumina is a stable and protective scale.

2.3.2 Laser Annealing. The system employed was a multi-beam continuous wave carbon dioxide laser with a maximum power of 500 W. A power of 80 W and speed of 1500 μ/s were chosen for the modification of the alumina-coated surface. It was carried out by directing the laser beam on the specimen and simultaneously scanning the beam from one end to the other in the X-direction by moving the specimen. The irradiation was repeated by moving the specimen in the Y-direction also.

2.4 Ion-Nitriding

Ion-nitriding is a method of surface modification with a view to harden the surface. In the present experiment the nitrogen irradiation of the stainless steel surface was carried out by using an accelerator. The samples were mounted on a copper block kept inside the vacuum chamber of the accelerator. These samples were irradiated with 100 keV ions of N_2^+ at room temperature. The beam current was kept at 0.009-0.011 μA/mm^2 to minimize heating effect. The fluence used was 5×10^{14} ions/mm^2. The duration of ion-irradiation was 21.6 ks. A surface nitrogen concentration of 0.16% was achieved by the present nitriding process.

2.5 The Oxidation Experiment

The specimens were kept in a furnace at 1123 K. It was weighed periodically. The total duration of oxidation was 3.6 Ms. At the end, the specimens were examined by various post-oxidation examinations such as Scanning Electron Microscopy (SEM), Energy Dispersive Spectroscopy (EDS) and x-ray Diffraction (XRD) in the glancing incidence mode.

3. Results and Discussion

3.1 Kinetics of Oxidation

The results of the mass gain experiment are shown in Fig. 1. The unmodified 316 LN SS exhibited the highest rate of

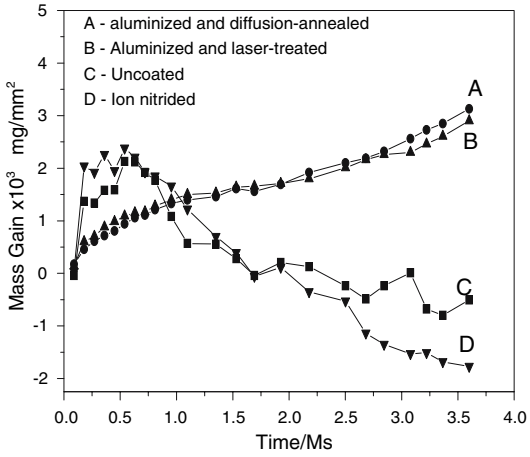

Fig. 1 Mass gain data of specimens oxidized at 1123 K

Table 1 Composition of 316 LN SS

Element	Cr	Ni	Mn	Si	Co	Mo	Cu	C	N
Mass %	18	10.5	1.35	0.6	0.2	2.0	0.25	0.02	0.1

oxidation. The initially formed scale was found to be not adherent and spalled to the extent so that the specimen even showed mass loss. The zigzag nature of the curve indicates that descaling has occurred after each time the scale has acquired a critical thickness. On the other hand, the alumina-modified specimen exhibited a uniform mass gain on oxidation commensurate with a parabolic rate behavior. Further more, the rate of oxidation was much lower than the bare specimen. Both the aluminized specimens (aluminized and diffusion-annealed and aluminized and laser treated) showed similar oxidation kinetics.

Nitridation did not result in the improvement in the oxidation behavior. However, nitridation enhanced the surface hardness from 250 VHN to 266 VHN without impairing the oxidation resistance.

The data on mass gain at specific intervals and the corresponding masses of the spalled oxide are listed in Table 2. The masses of the spalled oxide are maximum in the case of bare and nitrided specimens.

The aluminized specimen showed a marginal deviation from parabolic oxidation kinetics after 2.88 Ms of oxidation. It is presumed that the scale has undergone cracking and a stage of enhanced oxidation has set in on account of exposure of bare surface to air. Investigation by EDS revealed the existence of granular structures, which are regions of enhanced rate of oxidation and spallation.

3.2 Analysis of Surface by SEM and EDS

The uncoated specimen showed the generation of heterogeneous oxide scale (Fig. 2). The alumina-coated specimen showed the generation of Al_2O_3 on the surface (Fig. 3a). Both laser treatment and diffusion annealing showed identical protective behavior. The microstructure of the laser-treated specimen is shown in Fig. 4a. Nodular structures were observed on the surface in both the cases(Fig. 3b, 4b, respectively) indicating the onset of rapid growth and spallation of the scale. The SEM structure of nitrided specimen is given in Fig. 5.

Analysis by EDS indicated that the uniform layer in the oxidized bare stainless steel is predominantly iron oxide with minor concentration of chromium on the surface scale. The surface compositions of different specimens are listed in Table 3.

The uncoated specimen showed the generation of oxides of chromium and iron. The aluminized specimen after oxidation formed predominantly the oxide of aluminum at the surface. However, the analysis of the nodular region revealed that a large part of iron ions have diffused through the pre-existing scales and appeared as iron oxide at the surface. The high diffusion rate of iron compared to chromium and nickel, through pre-existing scale has been reported as the reason for this behavior (Ref 12, 13). The laser-treated specimen also showed similar compositional variation of oxide scale. The nitrided specimen showed preferential generation of oxide of chromium. Nitridation probably caused the enrichment of chromium on the surface due to the formation of nitrides of chromium (both CrN and Cr_2N are thermodynamically stable under present conditions). On subsequent oxidation these nitrides were converted to oxide. Iron does not form a stable nitride and hence has not segregated to the surface on nitridation. The presence of iron oxide at the surface is the result of high rate of diffusion of iron.

3.3 Characterization of Phases by Glancing Incidence X-ray Diffraction (GIXRD)

The oxides formed on the surface of the specimen were characterized by GIXRD using CuKα as the incident source. A glancing angle of 1° was employed. The oxide scales

Table 2 Data of mass gain and corresponding masses of the spalled oxide

	Mass gain, $\times 10^3$ mg/mm^2				Mass of spalled oxide, mg			
Time/Ms	1	2	3	4	1	2	3	4
0.09	−0.0384	0.174	0.136	0.034	0	0.053	0.017	0
0.18	1.37	0.457	0.603	2.04	0.454	0.159	0.167	0.701
0.27	1.34	0.612	0.707	1.92	0.680	0.211	0.231	0.911
0.36	1.58	0.72	0.880	2.26	1.215	0.275	0.302	1.11
0.45	1.59	0.805	0.984	1.95	1.65	0.318	0.375	1.30
0.54	2.13	0.940	1.09	2.38	2.04	0.416	0.456	1.65
0.63	2.12	1.06	1.15	2.21	2.32	0.506	0.55	1.89
0.72	1.92	1.11	1.17	1.93	2.56	0.584	0.634	2.14
0.81	1.77	1.21	1.28	1.85	2.8	0.642	0.711	2.37
0.954	1.08	1.33	1.40	1.66	3.16	0.745	0.837	2.83
1.098	0.569	1.4	1.5	1.22	3.57	0.837	0.964	3.21
1.35	0.557	1.46	1.53	0.698	3.95	0.964	1.11	3.62
1.53	0.282	1.61	1.64	0.395	4.28	1.05	1.26	3.95
1.692	−0.0384	1.56	1.66	−0.057	4.68	1.15	1.37	4.37
1.926	0.205	1.69	1.71	0.114	5.07	1.27	1.49	4.74
2.178	0.128	1.92	1.80	−0.35	5.41	1.40	1.63	5.06
2.502	−0.237	2.10	2.01	−0.527	5.83	1.56	1.81	5.49
2.682	−0.487	2.19	2.16	−1.14	6.26	1.70	1.96	5.87
2.844	−0.237	2.32	2.26	−1.35	6.70	1.83	2.11	6.30
3.078	0.012	2.56	2.30	−1.53	7.11	1.99	2.25	6.70
3.222	−0.679	2.73	2.46	−1.51	7.45	2.11	2.36	6.99
3.366	−0.800	2.85	2.61	−1.68	7.80	2.24	2.55	7.28
3.60	−0.506	3.13	2.90	−1.77	8.13	2.41	2.72	7.66

(1) Uncoated, (2) aluminized and diffusion annealed, (3) laser annealed, (4) nitrided

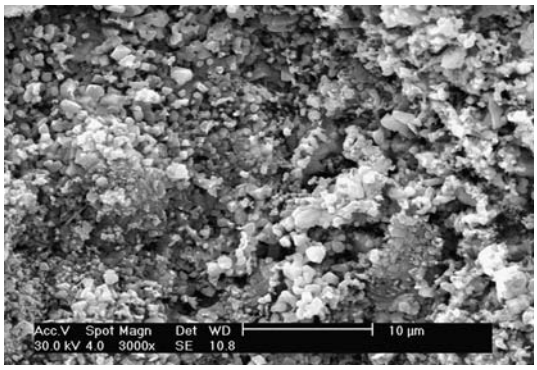

Fig. 2 SEM micrograph of oxidized specimen not subjected to surface modification

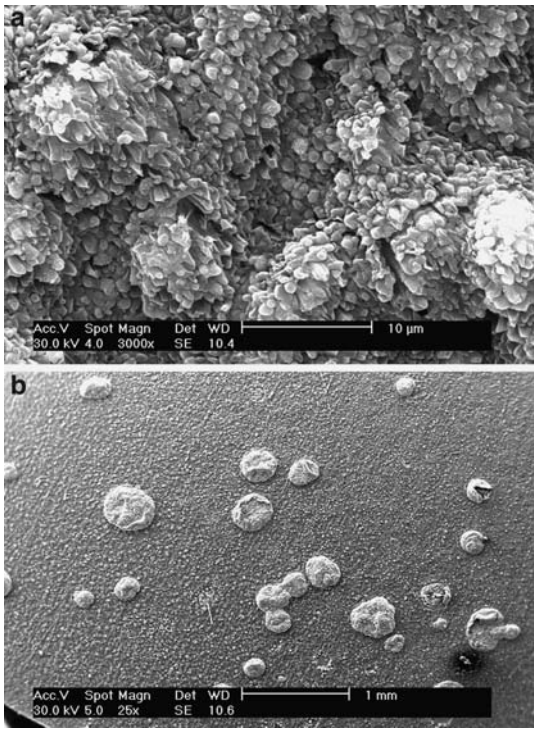

Fig. 3 (a) SEM micrograph of aluminized sample after oxidation for 3.6 Ms. Pre-treatment was carried out by heating at 873 K for 10.8 ks followed by 1173 K C for 90 ks. 3 (b) SEM micrograph of specimen aluminized and oxidized (nodular region)

spallen from various specimens were also analyzed. Typical results of the analyses are given in Fig. 6a to c and the identified phases corresponding to all the specimens are summarized in Table 4.

3.4 Mechanism of Nodular Growth and Scale Failure

When austenitic stainless steel is exposed to an oxygen-rich atmosphere, the protective scale expected to be developed is Cr_2O_3 as this is the most thermodynamically stable oxide among other constituents of stainless steel. For the alloy to sustain a continuous protective scale, the chromium content has to be in the range of 16-20% (Ref 14). If the chromium content is lower, the oxygen will encounter other elements present in the matrix such as iron, manganese and nickel. The transformation from a protective scale to a thicker scale has been

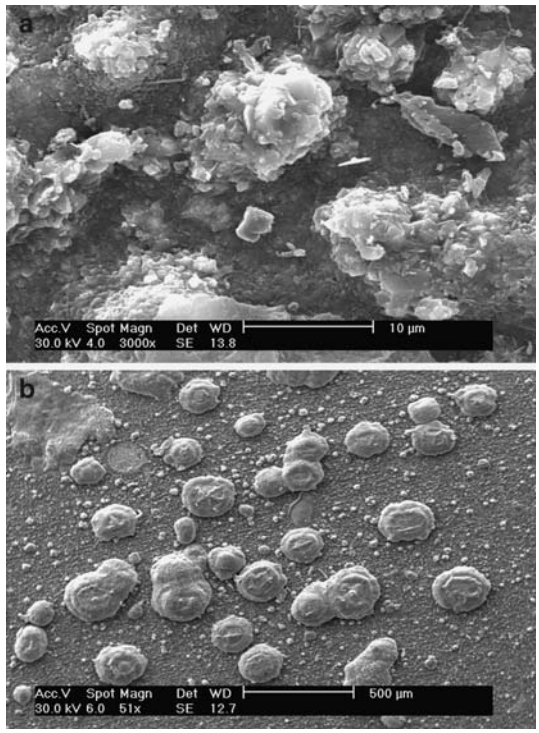

Fig. 4 (a) SEM micrograph of aluminized, laser annealed and oxidized specimen. (b) SEM microstructure of laser annealed and oxidized specimen showing nodular structure

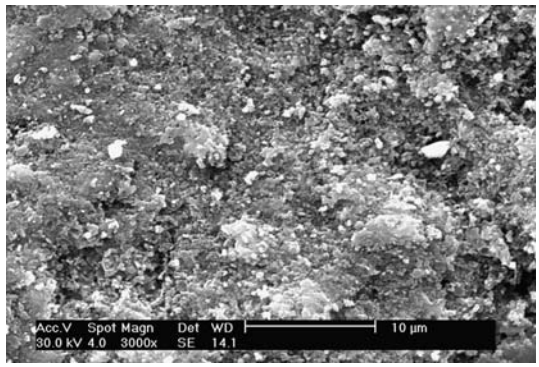

Fig. 5 SEM microstructure of nitrided specimen after oxidation

reported in the literature. Wood et al. (Ref 15) proposed two probable mechanisms for the generation of iron-rich nodules on the surface. The first mechanism takes into account the entry of iron and nickel into the Cr_2O_3 film and the subsequent transformation into a spinel structure. Second theory is based on the stress associated with the growth of the scale which ultimately leads to the cracking. The crack exposes the underlying layer and leads to rapid growth of iron-rich oxide. The nodular growth is proposed to be aided by both these processes. In the aluminized specimen the nodular region was enriched in iron and the nodules also showed the generation of cracks. Thus the present investigation gives supportive evidence to Wood's theory. The fast rate of diffusion of iron plays supportive role for the growth of nodular structure. Based on present results, the oxidation of stainless steel is proposed to proceed in three steps, viz;

Table 3 Surface composition of oxide scale

Sample	Composition, mass %
Uncoated	Cr = 24 Fe = 54.8 Ni = 19.96
Aluminized and pre-treated (uniform region)	Al = 84.61 Cr = 6.13 Fe = 3.64
Aluminized, diffusion annealed and oxidized (uniform region)	Al = 75.13 Cr = 5.98 Fe = 16.89
Aluminized, diffusion annealed and oxidized (nodular region)	Al = 4.33 Cr = 13.23 Fe = 77.87 Ni = 4.58
Aluminized, laser annealed and oxidized (uniform region)	Al = 78.51 Cr = 4.18 Fe = 15.69
Aluminized, laser annealed and oxidized (nodular region)	Al = 2.4 Cr = 19.36 Fe = 78.18
Nitrided and oxidized	Cr = 62.7 Fe = 35.6

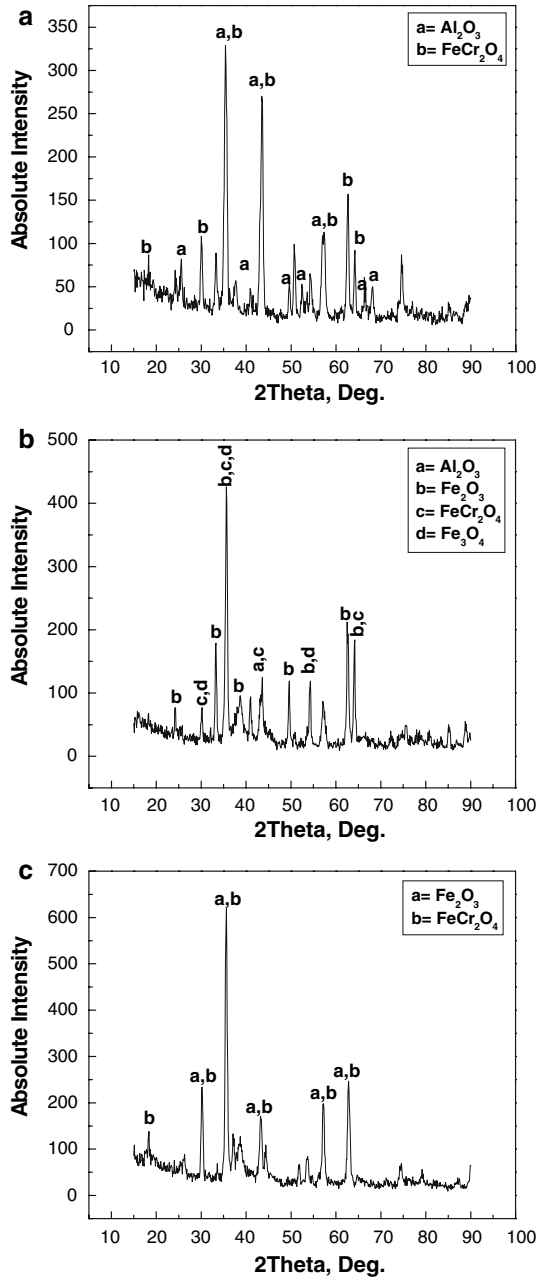

Fig. 6 (a) GIXRD spectra of thin film on the aluminized specimen after oxidation. (b) GIXRD spectra of thin film of laser-annealed specimen. (c) GIXRD spectra of thin film on the nitrided specimen

Table 4 GIXRD of oxide scale on the surface of the specimen and that spalled during the experiment

Specimens	Oxide phases
Uncoated	Cr_2O_3, $FeCr_2O_4$, Fe_2O_3
Spalled oxide from uncoated specimen	Fe_2O_3, Cr_2O_3, $FeCr_2O_4$
Aluminized specimen before oxidation	Al_5Fe_2, AlFe
Aluminized diffusion annealed and oxidized	Al_2O_3, $FeCr_2O_4$
Spalled oxide of aluminized specimen	Fe_2O_3
Aluminized, laser annealed and oxidized	Al_2O_3, Fe_2O_3, $FeCr_2O_4$, Fe_3O_4
Spalled oxide of laser treated specimen	Fe_2O_3
Nitrided and oxidized	Fe_2O_3, $FeCr_2O_4$
Spalled oxide from nitrided specimen	Fe_2O_3

(i) Generation of protective chromia scale
(ii) Penetration of the protective scale by fast diffusing ion such as that of iron. This results in the generation of nodules.
(iii) Nodules breaks and the oxide spalls. Ultimately nodules grow longitudinally and interconnect resulting in the generation of a uniformly oxidized surface. In the present investigation, the aluminized specimen (both diffusion annealed and laser annealed) attained the second stage of generation of nodular structure. On the other hand, both the bare and nitrided specimen attained the third stage of rapid oxidation followed by intermittent spallation.

The mass gain data and SEM data provides supportive evidence of the above mechanism.

4. Conclusion

Specimens of stainless steel 316 LN were subjected to oxidation at 1123 K in the as-received condition and after subjecting to surface modifications by different routes. The mass changes were measured periodically followed by post-oxidative examination at the end. The following conclusions are drawn from this investigation.

(i) Oxidation of stainless steel in the as-received condition resulted in rapid growth of scale followed by intermittent spallation.

(ii) Surface modification by deposition of aluminum resulted in significant improvement in oxidation resistance due to the formation of adherent alumina scale. Special heat treatment was required to promote the generation of adherent α-Al_2O_3 scale. Pre-treatment by diffusion annealing and laser treatment provided almost similar protective behavior.

(iii) For retarding the oxidation rate of iron-base alloys, it is necessary to device methods for reducing the diffusion rate of iron through the pre-existing scale.

(iv) Nitridation is a good method to improve the surface hardness without adversely altering the oxidation properties.

Acknowledgments

The authors wish to acknowledge the help rendered by Dr. V. Sankara Sasthry, Head XS&CGS Section, and MSD for XRD analysis, Dr. P. Shankar, MSD for physical vapor deposition and Mrs. R. Radhika for metallurgical analysis. The authors are also thankful to Dr. V.S. Raghunathan, AD, MCG for encouragement during the course of the work.

References

1. A. Paul, S. Elmrabet, F.J. Ager, J.A. Odriozola, M.A. Respaldiza, M.F. Da Silva, and J.C. Soares, Influence of Pre-Oxidation and Annealing Treatments on the Thermal Oxidation in Air at 1173 K of Cerium Implanted EN 1.4301 Stainless Steel, *Oxid. Met.*, 2002, **57**(1-2), p 33–51
2. W. Kaysser, Surface Modification in Aerospace Application, *Surface Eng.*, 2001, **17**(4), p 305–312
3. S.S. Patil, R.P. Fernandes, N.K. Patel, P.A. Rayjada, P.M. Raofe, and D.C. Kothari, Corrosion Resistance Study of Argon Ion Implanted and Ion Beam Mixed 316 SS, *Surface Coating Technol*, 2005, **196**(1-3), p 284–287
4. M. Saito, Y. Ishikawa, K. Ikeda, and H. Furuya, Oxidation Behaviour of Stainless Steel for Fast Breeder Reactor Fuel Cladding, *Nucl. Sci. Tech.*, 1984, **21**(5), p 356–365
5. R. Kossowsky, *Surface Modification Engg*, Vol. II, CRC Press Inc., Boca Raton, Florida, USA, 1989, p 174–209 and 257–284
6. S. Rajendran Pillai, Life History of Oxide Scale in Metals and Alloys, *Corrosion Rev.*, 2005, **23**(4-6), p 277–328
7. A. Andoh, S. Taniguchi, and T. Shibata, High Temperature Oxidation of Al-Deposited Stainless Steel Foil, *Oxid. Met.*, 1996, **46**(5-6), p 481–502
8. H. Echsler, D. Renusch, and M. Schuetze, Bond Coat Oxidation and its Significance for Life Expectancy of Thermal Barrier Coating System, *Mater. Sci. Tech.*, 2004, **20**, p 307–318
9. I. Gurappa, Identification of Hot Corrosion Resistant MCrAlY Based Bond Coating for Gas Turbine Engine Applications, *Surface Coating Technol.*, 2001, **139**(2-3), p 272–283
10. R. Mevrel, C. Duret, and R. Pichoir, Pack Cementation Processes, *Mater. Sci. Tech.*, 1986, **21**, p 201–206
11. M.J. Bennet and A.T. Tuson, Improved High Temp. Oxid. Behaviour of Alloys by Ion Implantation, *Mater. Sci. Eng. (A)*, 1989, **116**, p 79–87
12. S. Rajendran Pillai, P. Shankar, and H.S. Khatak, Cyclic Oxidation of P91 at 1073, 1123 and 1173 K, *High Temp. Mater. Processes*, 2004, **23**(3), p 195–204
13. M.H. Langrange, A.M. Huntz, and J.H. Davidson, The Influence of Y, Zr & Ti Addition on the High Temperature Oxidation Resistance of Fe-Ni-Cr-Al Alloys of Variable Purity, *Corros. Sci.*, 1984, **24**(7), p 613–627
14. R. Hales, The High Temperature Oxidation Behaviour of Austenitic Stainless Steels, *Werkstoff. Korros.*, 1978, **29**, p 393–399
15. G.C. Wood, M.G. Hobby, and B. Vaszko, Electron Probe Microanalysis of a Nodular Scale Growth on the Austenitic Stainless Steels, *J. Iron Steel Inst.*, 1964, **202**, p 685–695